# Energy and fluxes of thermal runaway electrons produced by exponential growth of streamers during the stepping of lightning leaders and in transient luminous events

Sebastien Celestin[1] and Victor P. Pasko[1]

Received 1 November 2010; revised 11 December 2010; accepted 6 January 2011; published 11 March 2011.

[1] In the present paper, we demonstrate that the exponential expansion of streamers propagating in fields higher than the critical fields for stable propagation of streamers of a given polarity leads to the exponential growth of electric potential differences in streamer heads. These electric potential differences are directly related to the energy that thermal runaway electrons can gain once created. Using full energy range relativistic Monte Carlo simulations, we show that the exponential growth of potential differences in streamers gives rise to the production of runaway electrons with energies as high as ~100 keV, with most of electrons residing in energy range around several tens of keVs. We apply these concepts in the case of lightning stepped leaders during the stage of negative corona flash. The computation of electric field produced by stepped leaders demonstrates for the first time that those energetic electrons are capable of further acceleration up to the MeV energies. Moreover, the flux of runaway electrons produced by streamers suggests that stepped leaders produce a considerable number of energetic electrons, which is in agreement with the number of energetic photons observed from satellites in terrestrial gamma ray flashes (TGFs). The results suggest that previously proposed process of relativistic runaway electron avalanche is difficult to sustain in the low-electric fields observed in thunderclouds and is generally not needed for explanation of TGFs. The present work also gives insights on relations between physical properties of energetic electrons produced in streamers and the internal electrical properties of streamer discharges, which can further help development and interpretation of X-ray diagnostics of these discharges.

**Citation:** Celestin, S., and V. P. Pasko (2011), Energy and fluxes of thermal runaway electrons produced by exponential growth of streamers during the stepping of lightning leaders and in transient luminous events, *J. Geophys. Res.*, *116*, A03315, doi:10.1029/2010JA016260.

## 1. Introduction

[2] Terrestrial gamma ray flashes (TGFs) are high-energy photons originating from the Earth's atmosphere in association with thunderstorm activity. TGFs were serendipitously recorded by BATSE detector aboard the Compton Gamma-Ray Observatory initially launched to perform observations of celestial gamma ray sources [*Fishman et al.*, 1994]. These events have also been detected and further studied by the Reuven Ramaty High Energy Solar Spectroscopic Imager (RHESSI) satellite [*Smith et al.*, 2005], the Astrorivelatore Gamma a Immagini Leggero (AGILE) satellite [*Fuschino et al.*, 2009; *Marisaldi et al.*, 2010], and the Fermi Gamma-ray Space Telescope [*Fishman and Smith*, 2008; *Briggs et al.*, 2010]. In addition to these space-based measurements, X-ray and gamma ray bursts have also been observed recently during natural and rocket-triggered lightning discharges [*Moore et al.*, 2001; *Dwyer et al.*, 2003, 2004a, 2004b, 2005; *Saleh et al.*, 2009]. The observed X-ray and gamma ray bursts have been linked to the production of high-energy electrons, so-called runaway electrons, in the Earth's atmosphere [*Fishman et al.*, 1994]. The recent research efforts on comparisons between gamma ray flashes observed from satellites and simulations of the propagation of energetic photons in the atmosphere have converged toward a source of photons with typical bremsstrahlung spectra located between ~15 and ~20 km altitudes, with a likely broad-beam geometry [*Dwyer and Smith*, 2005; *Carlson et al.*, 2007; *Østgaard et al.*, 2008; *Grefenstette et al.*, 2008; *Hazelton et al.*, 2009].

[3] Numerous experimental and theoretical works have strongly confined the conditions in which a TGF can occur [e.g., *Cummer et al.*, 2005; *Dwyer and Smith*, 2005; *Stanley et al.*,

[1]Department of Electrical Engineering, Communications and Space Sciences Laboratory, Pennsylvania State University, University Park, Pennsylvania, USA.


0148-0227/11/2010JA016260

2006; *Dwyer*, 2008; *Grefenstette et al.*, 2008; *Shao et al.*, 2010; *Smith et al.*, 2010]. In particular, *Stanley et al.* [2006] have correlated TGFs with normal polarity intracloud lightning that transports negative charges upward inside a cloud (+IC), and more recently, TGFs were found to occur within the initial development of +IC flashes [*Shao et al.*, 2010; *Lu et al.*, 2010]. However, the exact underlying mechanisms of the production of energetic electrons leading to the production of observed X-rays or gamma rays are not known.

[4] Runaway electrons were discussed by *Gurevich* [1961] and were defined by *Kunhardt et al.* [1986], who stated "an electron is runaway if it does not circulate through all energy states available to it at a given $E/N$, but on average moves toward high-energy states." The runaway phenomenon is a result of decreasing probability of electron interactions with atomic particles for electrons with energies in the range from ~100 eV to ~1 MeV [*Gurevich*, 1961]. In recent years, the thermal runaway electron process, accelerating cold electrons to high energies by extremely high electric fields [e.g., *Moss et al.*, 2006], has become a more and more convincing mechanism for production of TGFs as compared to the mechanism of runaway breakdown initiated by relativistic electrons generated by cosmic rays [e.g., *Gurevich et al.*, 1992; *Gurevich and Zybin*, 2001; *Gurevich et al.*, 2004; *Gurevich and Zybin*, 2005; *Roussel-Dupré et al.*, 1994; *Dwyer*, 2003]. In fact, it has been found that TGFs observed from satellites cannot be produced by relativistic runaway electron avalanches originating from background radiation or extensive cosmic ray air showers alone [*Dwyer*, 2008]. However, the fluxes of runaway electrons from lightning leaders have been calculated to be insufficient to fully explain the measured intensities of TGFs from space, and further amplification from relativistic runaway breakdown has been invoked [e.g., *Carlson et al.*, 2009; *Dwyer et al.*, 2010].

[5] Streamers are filamentary discharges propagating as ionizing waves that represent a common electrical breakdown process at ground level atmospheric pressure. The enhancement of electric fields around tips of streamers is one of the unique naturally occurring circumstances in which fields reaching $\sim 10E_k$, where $E_k$ is the conventional breakdown threshold field defined by the equality of the ionization and dissociative attachment coefficients in air ($E_k \simeq 30$ kV/cm at ground level), can be dynamically produced and sustained for relatively extended periods of time. The ability of streamer tip fields to generate runaway electrons was identified and discussed in the literature over two decades ago [*Babich*, 1982 and references therein], and a new insight on this phenomenon has been given by recent laboratory experiments [*Dwyer*, 2008; *Rahman et al.*, 2008; *Nguyen et al.*, 2008, 2010]. Although the exact mechanism providing electrons with the required energy to run away in electric fields typical of the streamer zone of negative leaders has not yet been understood, it has been proposed that with total potential differences on the order of tens of MV available from lightning leaders, during a highly transient negative corona flash stage of the development of negative stepped leader, runaway electrons ejected from streamer tips near the leader head can be further accelerated to energies of several tens of MeVs, depending on particular magnitude of the leader head potential [*Moss et al.*, 2006]. Moreover, the current theories of transient luminous events occurring above cloud tops and termed blue and gigantic jets generally favor a phenomenological link between jet discharges and streamer zones of lightning leaders [*Krehbiel et al.*, 2008 and references therein], and it has been suggested that the thermal runaway electron process operating in leaders may contribute to the production of terrestrial gamma ray flashes from the jet discharges [*Moss et al.*, 2006]. This mechanism has been further supported by recent analysis indicating that peak fields in gigantic jets derived from spectrophotometric measurements [*Kuo et al.*, 2009] have been underestimated and are in fact high enough to generate runaway electrons [*Celestin and Pasko*, 2010b].

[6] The electric potential distribution in a streamer is directly related to the energy that runaway electrons emitted from the streamer head can gain. This potential distribution is therefore crucial for possibility of further acceleration of runaway electrons in the electric field produced by the lightning leaders. In this paper, we demonstrate that the potential differences, or 'potential drops', in the region of the streamer head increase exponentially as the streamer propagates, and for the first time, we show that this effect facilitates the emission of sufficiently energetic electrons right from the streamer tip so that their probability of collisions with the molecules of air is reduced enough to enable their further direct acceleration in the electric field produced by a lightning leader tip. We also show that the strength of the fluxes of runaway electrons emitted from streamers during the negative corona flash stage of negative leader propagation is consistent with that required to produce TGFs.

[7] Bidirectional lightning leaders, that initiate intracloud (IC) lightning discharges and propagate in relatively low ambient fields ~0.2 kV/cm in thunderclouds [e.g., *Marshall et al.*, 1996, 2001], develop electric potential differences in their heads with respect to the ambient potential on the order of tens of MV as they extend over distances of several kilometers. Although these potential differences are readily available in the Earth's natural environment, the high field regions of positive and negative lightning leaders normally are shielded by their respective streamer zones that prevent direct production and acceleration of thermal runaway electrons to MeV energies. The high fields in the vicinity of leader tips can only exist for stepped leaders of negative polarity during the very transient negative corona flash stage of their development. As will be demonstrated below in this paper these high fields are still much lower than is required for thermal electron runaway phenomena. During the negative corona flash stage the high fields capable of driving runaway electrons can only be realized in relatively compact region of space in streamer heads. Due to the streamer exponential expansion and the related growth of potential differences in the streamer head mentioned above, the individual streamer heads are capable of accelerating runaway electrons to energies up to 100 keV. These electrons are then capable of further acceleration and harvesting of the available potential energy (tens of MeV) in the leader tip. As will be demonstrated by results of the present work, the runaway electrons created in streamers at near ground air pressures can gain 100 keV energy in very compact regions of space on the order one centimeter. We will also demonstrate that the relativistic runaway electron avalanche multiplication process, which has an avalanche length ~50 m [*Gurevich and Zybin*, 2001], is generally not necessary for explanation of significant fluxes of runaway electrons with

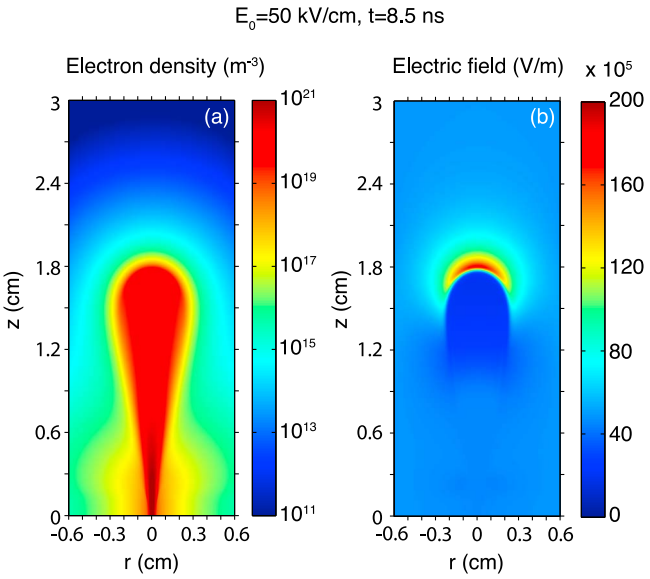


**Figure 1.** Cross-sectional views of (a) electron density and (b) electric field in a negative streamer simulated in air at ground pressure for a homogeneous applied electric field of 50 kV/cm at the time $t$ = 8.5 ns.

tens of MeV in the Earth's atmosphere responsible for production of TGFs.

[8] In section 2, we first illustrate the electric potential distributions in streamers that are investigated in the present study. We quantify the exponentially increasing potential differences in streamers by numerical simulations in section 3. Then, we demonstrate the impact of the high-potential differences on the energy that can be harvested by runaway electrons in section 4, and we discuss the results in section 5.

## 2. Potential Distributions in Streamers

[9] The propagation of streamers in homogeneous applied electric field $E_0$ higher than the stability field $E_s^{\pm}$ for propagation of streamers of a given polarity results in the continuous expansion of characteristic spatial dimensions in the streamer (radius, distance traveled or length, and the width of the charged layer in the head), as well as in increase of its velocity [*Kulikovsky*, 1995]. In fact, it has been demonstrated that the length of the streamer is proportional to its velocity [*Vitello et al.*, 1994], i.e., the streamer length increases exponentially in time. In a number of works, the radius of the streamer has been demonstrated to expand exponentially as well [*Naidis*, 1996; *Kulikovsky*, 1997a, 1997b; *Babaeva and Naidis*, 1997; *Kyuregyan*, 2008; *Liu et al.*, 2009]. Moreover, it is generally known that the maximum electric field in the streamer head stays approximately constant ($\simeq 5E_k$) during such an expansion under normal conditions of propagation because of the equality of the characteristic timescale of ionization and the dielectric relaxation (or Maxwell relaxation) time of the electric field in the streamer head [*Dyakonov and Kachorovskii*, 1988, 1989]. Therefore, under these conditions, one expects the electric potential differences, or drops, in the streamer head to increase exponentially as well.

[10] Figure 1 shows the electron density and electric field in a negative streamer simulated in air at ground level for a homogeneous applied electric field of 50 kV/cm at the time $t$ = 8.5 ns (the numerical model used to produce these results is described in section 3.1). The applied electric field exceeds the field of stable streamer propagation $E_s^- \simeq 12.5$ kV/cm [e.g., *Babaeva and Naidis*, 1997]. Figure 1 clearly shows the expansion of the streamer as it propagates in the simulation domain. The purpose of this section is to define and describe electric potential distributions in streamers on a conceptual level. The full details of the streamer model used to produce results in Figures 1 and 2 will be given in subsequent section 3.

[11] To illustrate the components of the electric potential distribution in a streamer, the scans of the electric potential and the electric field along the axis of symmetry in a negative streamer are shown in Figure 2. The negative streamer represented in Figure 2 is generated at ground pressure in an electrode gap of 3 cm. The cathode is set with a potential of −150 kV, while the anode is grounded (see Figure 2a). Therefore, as already mentioned above, the streamer propagates in a homogeneous electric field of 50 kV/cm (see Figure 2b). In Figures 2a and 2b, the region in which a significant charge density resides, when scanning along the axis of symmetry ($r$ = 0), is shaded. The maximum electric field appears right at the end of this zone. We define the potential drop in the streamer channel $\Delta U_c$ as the difference between the potential at $z$ = 0 and the potential at the left border of the significant charge density region. The potential drop in the streamer head $\Delta U_h$ is the difference between the potentials at the right and the left boundaries of the charged

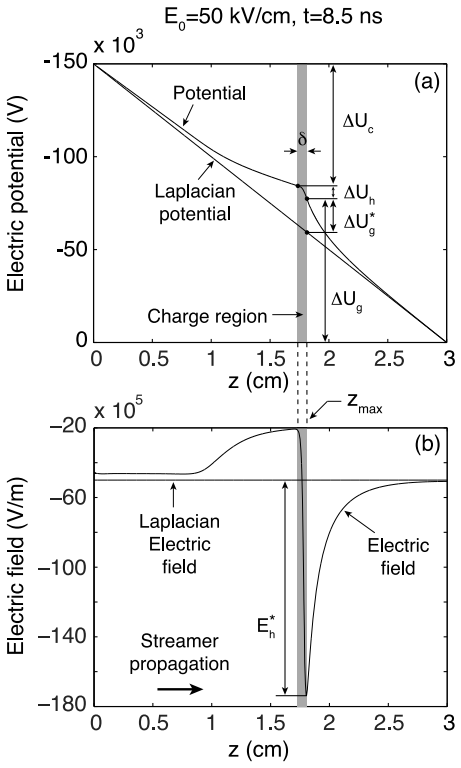


**Figure 2.** (a) Potential differences along the axis of symmetry in a negative streamer propagating in a plane electrode gap with a Laplacian applied electric field of $E_0$ = 50 kV/cm at $t$ = 8.5 ns. (b) Corresponding electric field along the axis of symmetry of the streamer.

density region. We also introduce the potential difference $\Delta U_g$ as the potential on the right boundary of the charged region minus the potential of the anode (see Figure 2a). In order to make quantitative estimates, one can consider the one-dimensional (1-D) Poisson's equation:

$$\frac{\partial^2 U}{\partial z^2} = -\frac{\rho}{\varepsilon_0} \tag{1}$$

where $U(z)$ is the electric potential along the axis of symmetry, $\rho$ is the charge density, and $\varepsilon_0$ is the permittivity of free space. Considering that the charge density is significant only in the streamer head, more precisely in the shaded region of size $\delta$ depicted in Figure 2, integration of (1) leads to

$$E_h^* = \int_\delta \frac{\rho}{\varepsilon_0} dz \equiv \frac{\overline{\rho}\delta}{\varepsilon_0} \tag{2}$$

where $E_h^*$ is the maximum of the space charge electric field in the streamer head, that is the maximum of the total electric field minus the applied Laplacian electric field, and $\overline{\rho}$ is the spatial average of $\rho$ defined in this relation. In the present work, we use the label "*" to represent space charge quantities as opposed to Laplacian (i.e., externally impressed) quantities. Note that a similar relation to equation (2) has been established by *Kulikovsky* [1997a]. One can determine the potential drop in the streamer head due to the space charge:

$$\Delta U_h^* = \int_\delta E dz \simeq \int_\delta \frac{\overline{\rho} z}{\varepsilon_0} dz = \frac{\overline{\rho}\delta^2}{2\varepsilon_0} = \frac{E_h^* \delta}{2} \tag{3}$$

The relation (3) clearly shows that for a constant $E_h^*$ and an exponentially increasing $\delta$, the potential drop in the streamer head would follow an exponential increase as well.

[12] It is interesting to note that one can define a characteristic charge $Q_h$ in the streamer head so that the relation $E_h^* = Q_h/(4\pi\varepsilon_0 R_s^2)$ is respected, where $R_s$ is the radius of the streamer. This leads to

$$Q_h = 4\pi\varepsilon_0 E_h^* R_s^2 \tag{4}$$

From $Q_h$ one can estimate the field $E_g^*$ in front of the streamer head as

$$E_g^*(z) = \frac{Q_h}{4\pi\varepsilon_0 (z - z_{max} + R_s)^2} \tag{5}$$

for $z > z_{max}$, where $z_{max}$ is the location of the maximum electric field. From equation (5), one can determine the drop of potential in the region ahead of the streamer $\Delta U_g^*$:

$$\Delta U_g^* = \int_{z_{max}}^{+\infty} E_g^* dz = \frac{Q_h}{4\pi\varepsilon_0 R_s} = E_h^* R_s \tag{6}$$

Similarly to the potential drop in the streamer head $\Delta U_h^*$, equation (6) shows that for an electric field approximately constant in the head, the exponential increase of the streamer radius leads to the exponential increase of the potential drop in the region ahead of the streamer $\Delta U_g^*$. The space charge potential differences $\Delta U_h^*$ and $\Delta U_g^*$ are related to the corresponding total potential drops $\Delta U_h$ and $\Delta U_g$ represented in Figure 2 as $\Delta U_h = \Delta U_h^* + \Delta U_h^L$ and $\Delta U_g = \Delta U_g^* + \Delta U_g^L$, respectively, where $\Delta U_{h,g}^L$ indicate the corresponding differences associated with the Laplacian electric potential. If the streamer propagates in a homogeneous electric field $E_0$, we have the relations: $\Delta U_h^L = E_0\delta$ and $\Delta U_g^L = U^L(z_{max})$. Despite the simplicity of the relations described above, we have observed that they accurately describe the potential drops in actual simulated streamers during their expansion.

[13] If one considers streamers propagating in an electrode gap, the relation (6) would remain valid as long as the streamer head is far from the electrode, i.e., $L - z_{max} > R_s$, where $L$ is the length of the electrode gap. When the streamer head gets close to the electrode, the relation (6) should be refined by including contribution from the image charges:

$$\Delta U_g^* \simeq \frac{Q_h}{4\pi\varepsilon_0}\left(\frac{1}{R_s} - \frac{1}{2(L - z_{max}) + R_s}\right) = E_h^* R_s - \frac{E_h^* R_s^2}{2(L - z_{max}) + R_s} \tag{7}$$

[14] We note that the direct inspection of Figure 2a can be used for understanding of the basic physical reason for the growth of potential difference in the streamer head. This growth can be linked to the fact that electric field in the streamer body is lower than the ambient applied electric field (as visually manifested in Figure 2a by smaller potential gradient in the streamer body in comparison with gradient of the Laplacian potential). In this regard, it is also useful to mention that streamers propagating in so-called stability fields for positive and negative streamers $E_s^{\pm}$, in which they do not accelerate, do not expand, and do not increase the potential differences in their heads, have electric fields in their bodies exactly equal to the ambient applied field (i.e., the stability field). In the same vein, the well developed streamers that form in a high field and then enter a region with applied field lower than the stability field very quickly decelerate and cease existence [*Babaeva and Naidis*, 1997].

## 3. Exponential Streamer Expansion

### 3.1. Streamer Model

[15] In order to simulate the dynamics of streamers, we use the drift-diffusion equations coupled with Poisson's equation [*Bourdon et al.*, 2007, equations (26)–(29)]. In this study, we consider the streamer propagation as purely axisymmetric. The transport and source parameters are taken from *Morrow and Lowke* [1997]. The drift of charged species is solved using a flux-corrected transport (FCT) method [see *Bourdon et al.*, 2007]. The photoionization is taken into account through the 3-Group $SP_3$ method derived by *Bourdon et al.* [2007] and *Liu et al.* [2007].

[16] The negative streamer is initiated by placing a Gaussian plasma cloud near the high-voltage cathode in a gap with planar electrodes separated by 3 cm, where the ambient electric field $E_0 = 50$ kV/cm ($\sim 1.5E_k$) is applied by setting the cathode to a potential of −150 kV and the anode to 0 V. We use a cylindrical computational domain $L \times R = 3$ cm × 0.6 cm, where $L$ and $R$ are axial and radial, respectively, dimensions. The domain is discretized using a numerical Cartesian grid with 3600 × 720 points. The initial Gaussian density is defined with a maximum of $n_0 = 10^{18}$ m$^{-3}$ with a

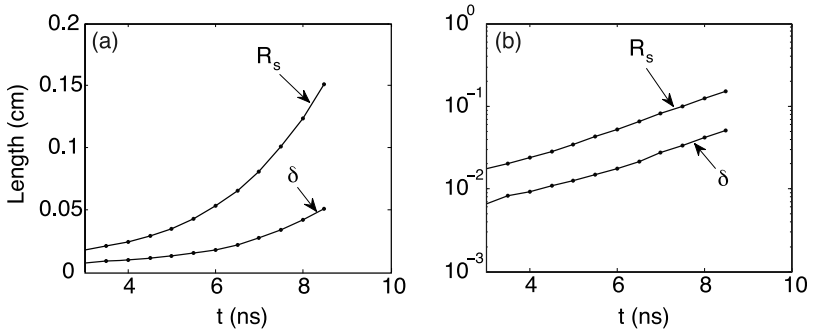


**Figure 3.** Radius $R_s$ and width of the space charge layer $\delta$ in a negative streamer propagating under an applied electric field of 50 kV/cm for a (a) linear scale and (b) semilog scale.

characteristic width of 0.1 mm, and the air density is chosen to be $N_0 = 2.688 \times 10^{25}$ m$^{-3}$, corresponding to the ground level. In the following, in order to extract the quantities $\Delta U_h$ and $\Delta U_g$, we first track the maximum of charge density $\rho_{max}$ and define the streamer head region as the region where $\rho > \rho_{max}/6$. The streamer head region being defined, we obtain the potential drops directly by computing differences of potential in numerical simulation results. Note that the factor 1/6 is chosen in order to obtain a good quantitative agreement with relations discussed in section 2. We have observed that varying this factor from 1/*e* to 1/10 only leads to slight changes in the results and do not affect the conclusions.

### 3.2. Streamer Expansion and Potential Drops

[17] From the simulation results, one can obtain the width of the space charge region $\delta$ and the radius of the streamer $R_s$. Concerning the latter, we have observed that relation (6) is especially convenient for determination of the radius of the streamer, since $\Delta U_g^*$ and $E_h^*$ are readily measurable from simulation results. This gives an accurate estimate of the electrodynamic radius of the streamer, that is defined by the three-dimensional shape of the charge density layer in the region of the streamer head. The time evolutions of $\delta$ and $R_s$ for the case of a negative streamer propagating under conditions of homogeneous electric field of 50 kV/cm are shown in Figure 3. The simulation results show that after an initial phase of formation, the streamer enters a continuous phase of exponential expansion. We note that similar results were already obtained for positive streamers by *Kulikovsky* [1997a]. For the results presented in Figure 3, a fit with an exponential function gives a characteristic growth time of $\delta$ and $R_s$ of approximately $\tau \simeq 2$ ns. It is interesting to note that both characteristic length $\delta$ and $R_s$ have the same growth rate. This demonstrates that the expansion of the streamer is homothetic. Moreover, the streamer length also grows exponentially in time with the same rate as $R_s$. Note that this effect is responsible for the characteristic expanding shapes of long streamers reported in Figure 1 of the present paper and by *Liu et al.* [2009, Figure 1].

[18] Relations (3) and (6) involve the characteristic length scales of streamers $\delta$ and $R_s$, respectively. Thus, the potential drop in the streamer head $\Delta U_h^*$ and the potential drop ahead of the streamer $\Delta U_g^*$ increase exponentially as well. Figure 4 represents the time evolution of the quantities $\Delta U_h^*$ and $\Delta U_g^*$ directly obtained from the simulation results of the same negative streamer using linear and semilog scales. The results presented in Figure 4 clearly demonstrate the exponential growth of $\Delta U_h^*$ and $\Delta U_g^*$ that follows initial phase of streamer formation. For the same case of applied field of 50 kV/cm, we calculate a time constant of approximately 2 ns corresponding to the exponential growth of $\Delta U_h^*$ and $\Delta U_g^*$ that agrees with the one found for $\delta$ and $R_s$. Having considered relations (3) and (6), this demonstrates the slow variation of the peak electric field in the streamer head.

### 3.3. Production of High-Electric Field in the Streamer Head

[19] Figure 4 demonstrates that potential drops in streamer get to very high values extremely fast during the streamer propagation. The propagation of the streamer discharge requires production of electrons downstream the streamer head. These electrons are believed to be produced by photoionization [e.g.,

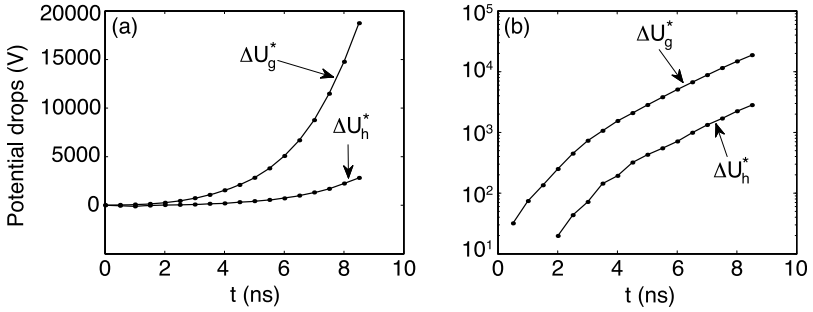


**Figure 4.** Potential drops in a negative streamer propagating under an applied electric field of 50 kV/cm for a (a) linear scale and (b) semilog scale.

*Bourdon et al.*, 2007 and references therein]. While the streamer expands exponentially, the length scale of photoionization, which is related to the absorption length of photons by oxygen molecules, remains constant. When the radius of the streamer reaches the order of magnitude of this UV photons absorption characteristic length, photoelectrons can no longer be created in front of the streamer head and the streamer can no longer propagate, finally leading to the branching of the streamer [*Liu and Pasko*, 2004]. While during the most of expansion dynamics of the streamer the maximum field in the streamer head stays close to $\sim 5E_k$, just prior to the branching of the streamer this peak field in the streamer head can reach very high values, and is even capable of exceeding the critical field for production of thermal runaway electrons $E_c \simeq 8E_k$ [*Moss et al.*, 2006]. Note that from the set of cross sections used in our Monte Carlo code (see section 4), we obtain $E_c \simeq$ 240 kV/cm at ground level.

[20] Although the very moment at which the streamer branches is difficult to determine in the framework of deterministic drift-diffusion equations, simulations of streamers show that branching is likely to happen when the radius of the streamer reaches several times the characteristic length scale of photoionization $(\chi_{\min} p_{O2})^{-1} \simeq 0.2$ cm at ground pressure in air [*Liu and Pasko*, 2004], where $\chi_{\min}$ and $p_{O2}$ are the absorption coefficient and the partial pressure of molecular oxygen, respectively. This effect of maximum radius before branching has been recently observed for positive sprite streamers along with the increase of the electric field and related optical output from the streamer head at the moment immediately preceding branching [*McHarg et al.*, 2010]. The maximum radius corresponding to negative streamers is believed to be much greater than in the positive streamer case [*Liu and Pasko*, 2004]. For the sake of simplicity, we define the value of the branching radius as $R_b = 0.5$ cm at ground pressure, which is a conservative estimate for negative and also for positive streamers based on numerical simulations [*Liu and Pasko*, 2004] and experimental observations [*McHarg et al.*, 2010]. Assuming that the streamer branches when its radius reaches $R_b = 0.5$ cm, and using the clear exponential trends depicted in Figure 3, one can accurately find the corresponding time of branching commencement $t_b \simeq 11.2$ ns and the corresponding streamer length $l(t_b) = 7$ cm. Additionally, because of the well established exponential growth of the potential drops in the streamers, one can accurately estimate $\Delta U_g^*(t_b) \simeq 86$ kV and $\Delta U_h^*(t_b) \simeq 12$ kV. In addition to ambient electric field, a runaway electron initiated at the position of the peak electric field in the streamer head will experience the potential difference $\Delta U_g^*(t_b)$ produced by the space charge of the streamer. For the considered model case of ambient electric field of 50 kV/cm, a runaway electron reaching a characteristic distance of one streamer radius from the streamer head would have undergone the significant difference of potential of $\Delta U_g \simeq 110$ kV. We note, however, that due to collisions with air molecules, even runaway electrons, for which the average friction force is reduced, cannot convert all of this potential energy into kinetic energy.

[21] It is generally believed that the steepness of the application of voltage in time has a strong impact on the development of the streamer zone of leaders [e.g., *Petrov and D'Alessandro*, 2002]. For the purpose of understanding the impact of the risetime of the applied voltage on the streamer dynamics, we have run simulations with applied voltages increasing in time. In the general case of streamer simulations, the applied voltage defines the ambient Laplacian field in which the streamer propagates (see section 3.1). In the particular study of the formation of streamer zones of negative leaders, this applied voltage corresponds to the electric potential generated by the leader during the negative corona flashes. We have observed that although the electric field in the streamer channel is not significantly affected by the variation of applied voltage, the electric field in the streamer head increases with the reduction in risetime of the applied voltage. By itself, this temporal variation of the applied voltage can make the electric field in the streamer head greater than the threshold for production of thermal runaway electrons without invoking the effect of relative increase of streamer head radius in comparison with photoionization length discussed above. In this case, the streamer and related electric potentials expand exponentially as well, or even over-exponentially since the ambient electric field is increasing. The simulations representative of conditions corresponding to negative corona flashes, that are using rise rates of applied voltages lower than 10 MV/30 ns (see section 5.1), show that streamers propagate over at least a few centimeters before the electric field in the streamer head becomes greater than $E_c$. Thus, we consider the potential differences in streamers given by the approach discussed in the previous paragraph as a good estimate of the potential differences in streamers after exponential expansion at the moment of production of energetic electrons. We emphasize that the exact relative contributions of the risetime of applied field and the expansion of the streamer head in comparison with the photoionization range to the production of a high field in the streamer head are not known and should be quantified in a separate dedicated investigation. We also suggest that the increase of the peak electric field in the streamer head due to the time derivative of the applied voltage plays a significant role in the recently observed dependence of X-rays production on the risetime of applied voltages in laboratory spark discharges [*March and Montanyà*, 2010].

[22] In section 4 we apply Monte Carlo simulations to accurately quantify the kinetic energies that runaway electrons can attain in the above discussed processes.

## 4. Energy of Runaway Electrons Produced by Expanding Streamers

### 4.1. Monte Carlo Model

[23] The Monte Carlo model we have developed simulates the propagation and collisions of electrons in air (80% $N_2$ and 20% $O_2$) under an applied electric field similarly to *Moss et al.* [2006]. This model is three-dimensional (3-D) in the velocity space, 3-D in the configuration space, relativistic, and simulates electrons from sub-eV to several MeVs [*Celestin and Pasko*, 2010a]. Excitation cross sections are taken from Bolsig+ database [*Hagelaar and Pitchford*, 2005] and are logarithmically extrapolated to high energies. The singly differential cross sections of ionization of $N_2$ and $O_2$ are calculated over the full range of energy through the relativistic binary-encounter-Bethe (RBEB) model [*Kim et al.*, 2000; *Celestin and Pasko*, 2010c]. The knowledge of this differential cross section allows for obtaining the energy of the secondary electrons [e.g., *Moss et al.*, 2006] after ionizing collisions. The scattering angles of primary and secondary electrons are then obtained from the relativistic

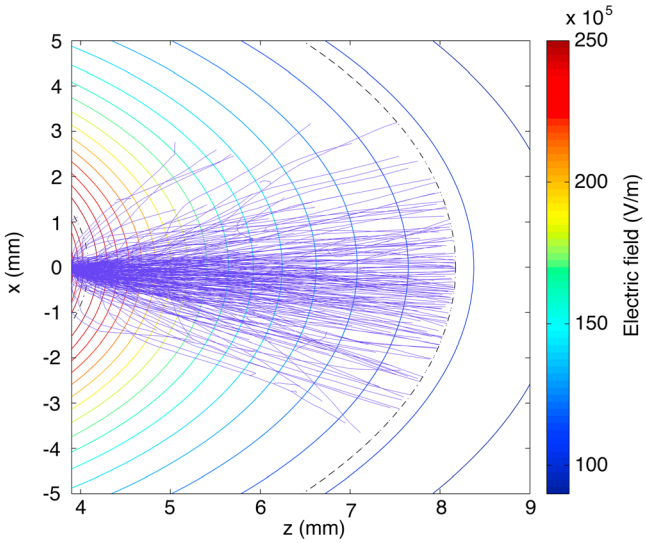


**Figure 5.** Trajectories of electrons with energies >1 keV obtained in one Monte Carlo simulation and configuration of applied electric field. The dotted-dashed line on the left represents the peak electric field in the streamer head $E_{\mathrm{ref}}$ = 260 kV/cm, and the dotted-dashed line on the right represents the locus of points at a distance $R'_{\mathrm{s}} = 0.41$ cm of the peak electric field, which is taken as a surface of reference for presentation of energy distribution of runaway electrons shown in Figure 6.

equations of conservation of momentum and energy considering than the newly formed ion is static. The scattering angles of any other collision than ionization are calculated from the differential cross sections documented by *Shyn et al.* [1972] and *Kambara and Kuchitsu* [1972] for energies lower than 500 eV. For higher energies, we use an analytical modified Rutherford differential cross section [*Moss et al.*, 2006, equation (17)] that gives satisfactory agreement with the usual relativistic multiple scattering formulation [e.g., *Lehtinen et al.*, 1999, equation (13)].

[24] Although elastic collisions do not play a significant role in the electron energy losses, they are numerous enough to have a significant impact on the angular scattering of electrons [e.g., *Lehtinen et al.*, 1999; *Dwyer*, 2010]. Elastic cross sections are extrapolated for energies greater than 10 keV using a screened Rutherford cross section as described by *Murphy* [1988]. The results given by the present full energy range Monte Carlo model have been successfully compared [*Celestin and Pasko*, 2010a] with results from intermediate energy models [e.g., *Hagelaar and Pitchford*, 2005], purely high-energy models [*Celestin and Pasko*, 2010c], and recent full energy range models [*Colman et al.*, 2010]. For the sake of brevity, these comparisons are not included in the present work, and will be covered in a separate dedicated publication.

### 4.2. Peak Kinetic Energy of Runaway Electrons

[25] We note that our analysis presented in section 3 allows to estimate accurately the potential differences and streamer head dimensions preceding the streamer branching. However, as already noted in section 3.3, the exact morphology of the streamer head just prior to branching is difficult to model realistically in the framework of deterministic drift-diffusion equations. In our Monte Carlo formulation, we approximate field distributions prior to branching using energy conservation considerations.

[26] In order to conserve energy during the increase of the electric field prior to the branching process, the potential differences in the streamer should stay constant. When formulating input electric fields used in Monte Carlo simulations, this consideration ensures that no artificial increase of the electric potential differences occurs, despite the increase of the peak electric field. Thus, considering that the magnitude of the peak electric field reaches a sufficient value for generating runaway electrons from the streamer tip, that is $E_{\mathrm{ref}}$ = 260 kV/cm ($\gtrsim E_{\mathrm{c}}$), one can easily calculate realistic $\delta$ and $R_{\mathrm{s}}$ at this moment: $\delta' = 2\Delta U^{*}_{\mathrm{h}}(t_{\mathrm{b}})/(E_{\mathrm{ref}} - E_0) \simeq 0.12$ cm and $R'_{\mathrm{s}} = \Delta U^{*}_{\mathrm{g}}(t_{\mathrm{b}})/(E_{\mathrm{ref}} - E_0) \simeq 0.41$ cm. In this way, we formulate the configuration of electric field when the streamer starts emitting runaway electrons and we can simulate the realistic dynamics of electrons in this system (see Figure 5).

[27] Figure 5 illustrates the mechanism of emission of thermal runaway electrons from the streamer tip. The initial electrons with energy 1 eV are regularly injected at a rate of $1.6 \times 10^{15}$ s$^{-1}$, at the location $z = R'_{\mathrm{s}} - 0.02$ cm = 0.39 cm (see Figure 5) on the axis of symmetry of the streamer. The reported results are not sensitive to the specific value of the initial low energy of electrons. At this location the electric field is approximately 227 kV/cm, that is insufficient for electrons to run away. The choice of this particular location is made for convenience, since, while drifting in the electric field, electrons have enough time to attain the thermal equilibrium before the first runaway electrons appear. The streamer field is static in the results we present in this paper. We have verified that taking into account a moving electric field in the simulations does not change the mechanisms we present in this paper, although it introduces the phenomenon of self-acceleration, which increases the maximum energy possibly gained by electrons by a few of keVs [*Babich*, 1982; *Moss et al.*, 2006]. While it does not bring a new insight on specific effects discussed in the present paper, we generally note that moving electric field configurations are difficult to simulate accurately since the velocity of streamers prior to and during branching is not accurately known [e.g., *Liu and Pasko*, 2006, Figure 7].

[28] As discussed above, the electric field and the corresponding potential difference that an electron experiences has a space charge component and a Laplacian component. Without accounting for the self-acceleration mechanisms, we have calculated above that an electron running away from the streamer head and traveling over a distance of one streamer radius (either $R_{\mathrm{s}} = 0.5$ cm or $R'_{\mathrm{s}} \simeq 0.41$ cm), experiences a difference of potential of $\Delta U_{\mathrm{g}} \simeq 110$ kV, and therefore the maximum energy possible for such an electron is 110 keV. This energy is not possibly reachable by electrons because of the numerous collisions they experience with molecules of air. However, because of their reduced probability of collision, the energy extracted by runaway electrons can approach this upper limit. In fact, the highest energy of runaway electrons after propagation over the distance $R_{\mathrm{s}}$ obtained in the simulation corresponding to the situation of Figure 5 is approximately 100 keV. In order to quantify the dynamics of runaway electrons after emission and acceleration from the streamer tip, we calculate the energy distribution function at a reference distance $R'_{\mathrm{s}} \simeq 0.41$ cm from the position of the peak

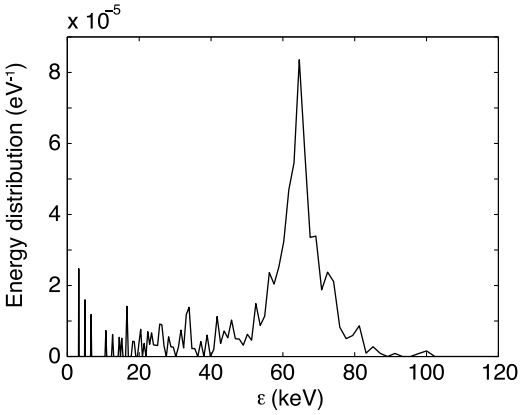


**Figure 6.** Energy distribution function of runaway electrons crossing the surface located at a distance of one streamer radius from the position of the peak electric field (see Figure 5).

electric field (shown by dotted-dashed line on the right-hand side of Figure 5). This result is presented in Figure 6.

[29] Figure 6 shows that despite the fact that the maximum energy can be approximately 100 keV, most of the runaway electrons obtain an energy close to ~65 keV, which represents an efficiency of conversion of the available electric potential energy of ~60%. This tremendous energy of runaway electrons emitted from the streamer tip is acquired by electrons on a timescale of a fraction of nanosecond. In section 5, we show that the 65 keV energy gained by runaway electrons from the emission process from streamer tips is high enough for their further acceleration in fields produced by lightning stepped leaders during negative corona flashes.

## 5. Discussion

### 5.1. The Necessity and Critical Role of Streamers

[30] While the propagation of a positive lightning leader is usually continuous, the propagation of a negative lightning leader usually shows a stepwise dynamics [*Bazelyan and Raizer*, 2000, p. 10]. Although details are not fully understood, one of the key components of the stepping process is the formation of a "space leader", which originates near the boundary of the streamer zone created by the previous leader step [*Bazelyan and Raizer*, 2000, p. 197]. During the connection between the main leader and the space leader, the electric potential of the new leader step increases extremely fast giving rise to a flash of a new negative streamer corona, the so-called "negative corona flash" [*Bazelyan and Raizer*, 2000, p. 199].

[31] Although very fast, the increase of electric field in front of the new leader branch is not instantaneous. In fact, the shortest timescale related to this process is on the order $\tau_E = l_b/c_r$, where $l_b$ is the length of the new leader branch, or step length, and $c_r$ is the propagation speed of the wave of electric potential in the new leader branch, which can be approximated by the propagation speed of a return stroke. The characteristic length of the new leader branch is $l_b \gtrsim 10$ m, and $c_r$ is close to the speed of light [e.g., *Rakov and Uman*, 2003, Table 1.1]. Therefore, the timescale of the increase of electric field in front of the new leader branch must be longer than $\tau_E \simeq 30$ ns.

[32] Because of the exponential multiplication of electrons in electric fields higher than $E_k$, high-electric fields cannot persist for a long time. Indeed, as the conductivity of air $\sigma$ is exponentially increasing for such fields, the characteristic timescale of screening of the electric field by the charges induced in a conducting medium, namely the Maxwell relaxation time $\varepsilon_0/\sigma$, exponentially decreases. Once the Maxwell time is shorter than the characteristic ionization time, the increase of the electron density can no longer proceed, and the electric field is significantly screened, as it is in streamer heads [*Dyakonov and Kachorovskii*, 1988, 1989]. Thus, in order to obtain an estimate of the maximum timescale over which a given electric field can exist, one can consider conditions when the Maxwell time becomes equal to the ionization time for several given magnitudes of a homogeneous electric field $E_0$ in air in a uniform and infinite space. Assuming that the mobility of ions is negligible compared to the mobility of electrons, we have $\sigma \simeq q_e n_e \mu_e$, where $q_e$, $n_e$, and $\mu_e$ are the elementary charge, the electron density, and the electron mobility, respectively. We consider the exponential increase of the electron density:

$$n_e = n_{e0} \exp[(\nu_i - \nu_{2b} - \nu_{3b})t] \tag{8}$$

where $\nu_i$, $\nu_{2b}$, and $\nu_{3b}$ are, respectively, the ionization frequency, the two-body attachment frequency, and the three-body attachment frequency corresponding to a given electric field $E_0$. These frequencies are calculated from the coefficients given by *Morrow and Lowke* [1997]. Since we only seek an order of magnitude estimate of the critical time $\tau_c$ over which an electric field can be sustained, it is assumed that the trend of the electron density is purely exponential (see equation (8)), that is feedback screening effects of electrons on the applied electric field are not taken into account. More elaborate descriptions are feasible and would result in the characteristic inception time of streamers [*Raizer* 1991, section 12.3.2]. In this way, we can easily find the time for which the Maxwell time is equal to the ionization time $1/\nu_i$, i.e., $\varepsilon_0/\sigma = 1/\nu_i$, for a specified electric field $E_0$. This critical time $\tau_c$ along with the corresponding electric field is presented in Figure 7. To calculate the results shown in Figure 7, we have chosen an initial ambient electron density of $n_{e0} = 1$ cm$^{-3}$. Since the Maxwell time decreases exponentially, various initial ambient electron densities result in very close critical times. Indeed, we have verified that multiplying the initial electron density by one thousand only leads to variations of $\tau_c$ on the order of 30%. We have also verified that the effect of nonsimilar scaling with atmospheric density due to the three-body attachment does not affect results presented in Figure 7, and therefore we consider that the result presented in Figure 7 is scalable with air density $N$ as $\tau_c \sim 1/N$ and $E_0 \sim N$. These considerations are important for relevant estimates at different altitudes in the Earth's atmosphere.

[33] Figure 7 shows that electric fields higher than 100 kV/cm (~$3E_k$) cannot be sustained over more than the nanosecond timescale at ground pressure. In fact, Figure 7 shows that the maximum electric field that can be sustained over the timescale of increase of the electric field $\tau_E \simeq 30$ ns due to the connection between the new leader branch and the main lightning leader is

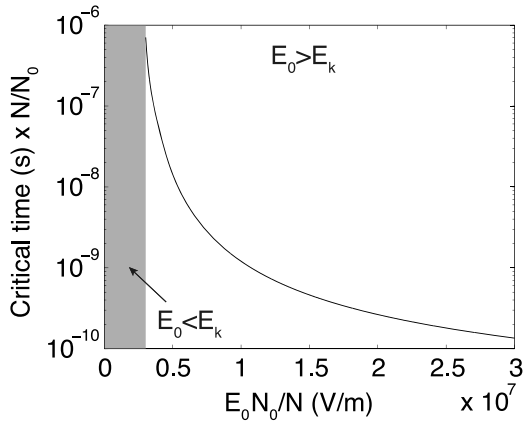


**Figure 7.** Maximum time over which a given electric field $E_0$ can be sustained.

approximately $E_0$ = 50 kV/cm. The thermal runaway electron threshold being $E_c \simeq 240$ kV/cm, it implies that the field generated by the leader during a negative corona flash is insufficient to produce runaway electrons on its own. However, the powerful streamer zone which is developed during this process on the microsecond timescale is able to generate thermal runaway electrons [*Moss et al.*, 2006]. This shows that the production of streamers, that dynamically produce and sustain high fields $\gtrsim E_c$ in small volumes around their heads, is required as a necessary stage for production of energetic electrons from natural stepping lightning leaders, and the physical characteristics of streamer discharges have to be studied in order to quantify the properties of those energetic electrons. Moreover, the preceding analysis shows that the results obtained in section 4.2 using results on negative streamers propagating in an ambient electric field $E_0$ = 50 kV/cm are consistent with the dynamics of streamers forming the streamer zone of negative lightning leaders during negative corona flashes.

### 5.2. Acceleration and Flux of Energetic Electrons in the Leader Field

[34] Modeling the full dynamics of a leader is beyond the scope of the present paper. However, the discussion of a few physically representative quantities is insightful. The application of the method of moments [*Balanis*, 1989, p. 670] allows for computing the electric field generated by an equipotential perfectly conducting leader channel immersed in an ambient thundercloud electric field. In the present study, we consider the negative part of a bidirectional lightning leader representative of a positive intracloud lightning (+IC); that is, the negative stepped leader is propagating upward. Using a characteristic leader length of $l_l$ = 1 km, the negative leader is considered to be propagating in a low-ambient electric field $E_{amb}$ = 0.2 kV/cm, which is close to the magnitudes of electric fields usually observed in thunderclouds [e.g., *Marshall et al.*, 1996, 2001]. Because of the length of the modeled leader and the magnitude of the ambient electric field, the total potential differences between respective positive and negative leader heads and ambient potential are of magnitude $U_l \simeq l_l E_{amb}/2$ = 10 MV [see *Bazelyan and Raizer*, 2000, p. 54], which is in good agreement with typical characteristics of lightning stepped leaders [e.g., *Rakov and Uman*, 2003, Table 1.1]. Choosing a leader radius of 1 cm [*Rakov and Uman*, 2003, p. 134], and using the method of moments [*Balanis*, 1989; *Riousset*, 2006], one obtains the one-dimensional electric potential and field along the axis of symmetry, representing the potential and field produced by a negative leader during the corona flash, as depicted in Figure 8. In the application of the method of moments, a 1 km long cylindrically symmetric channel with radius of 1 cm is assumed to be perfectly conducting and equipotential. The solution allows accurate calculation of the electric charge distribution induced on the channel due to application of external homogeneous field $E_{amb}$, and accurate reconstruction of three-dimensional electric field distribution of positive and negative ends of the channel. We note that during most of the time of advancement of positive and negative leader heads, the extremely high fields around their tips are shielded by the formation of corresponding positive and negative streamer zones with effective radii $R_{sz}^{\pm} = U_l/2E_s^{\pm}$ [*Bazelyan and Raizer*, 2000, p. 69], where $U_l$ is the magnitude of potential difference formed by the leader head with respect to ambient potential ($U_l \simeq l_l E_{amb}/2$). The considered vacuum solution does not account for the streamer zone effects and is accurate only during the transient negative corona flash stage of negative leader development when negative leader head

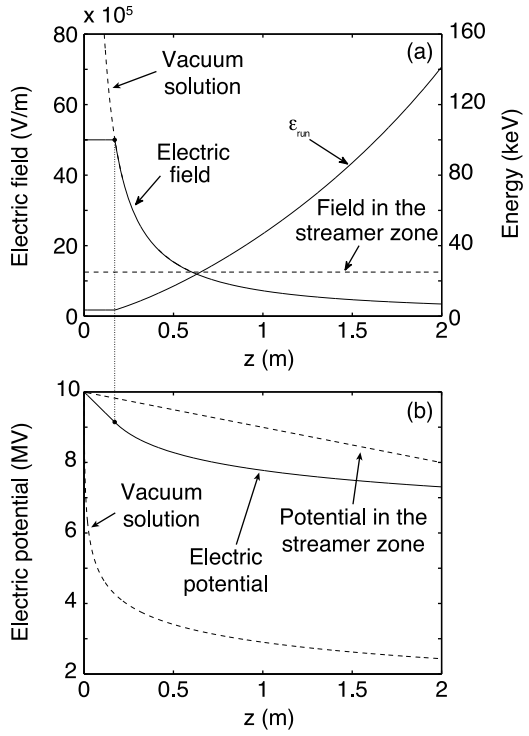


**Figure 8.** (a) Characteristic magnitude of the free space electric field calculated using the methods of moments produced by a perfectly conducting leader branch of 1 km length with a radius of 1 cm immersed in an ambient thundercloud electric field of 0.2 kV/cm. The corresponding minimum energy for thermal runaway electrons $\varepsilon_{run}$ is also shown. When the streamer zone is formed, the electric field in this region is approximately 12.5 kV/cm. The leader tip is located at $z$ = 0. (b) Corresponding electric potential produced by the leader (total electric potential minus ambient potential) during the negative corona flash and when the streamer zone is formed.

becomes temporarily partially unshielded (Figure 8), which is of primary interest in our present work. We account for finite time $\tau_E \simeq 30$ ns required for establishment of the new equipotential section of the leader. In particular, the electric field higher than the maximum sustainable electric field during $\tau_E \simeq 30$ ns (50 kV/cm) is represented in Figure 8a by the plateau between 0 and ~15 cm, and the corresponding linear potential in Figure 8b.

[35] Extrapolating the exponential variation of the streamer length we obtained in section 4.2, indicates that the branching would occur for a streamer of approximate length $l(t_b) = 7$ cm (see section 3.3). Considering this distance from the leader tip and the time taken to reach this location ($t_b \simeq 11.2$ ns) shows that the minimum required energy $\varepsilon_{run}$ for an electron to further accelerate, i.e., to become a runaway electron [e.g., *Moss et al.*, 2006, Figure 2], is defined by the electric field of ~50 kV/cm, and is equal to $\varepsilon_{run} \simeq 3.5$ keV. The values of $\varepsilon_{run}$ at different distances from the leader tip and corresponding electric field values are included in Figure 8a. Thus, one sees that electrons with energy calculated for streamers without accounting for their exponential growth, that is ~2 keV [*Moss et al.*, 2006], cannot become runaway electrons in this system and will be unable to gain much energy. However, from our present study it is obvious that the typical 65 keV electrons obtained in section 4.2, that continue to runaway in fields $\geqslant$6 kV/cm, will have space and time to further accelerate to energies of several MeVs given the potential differences available in the electric field produced by the leader tip.

[36] In Figure 8a, we also represent the electric field in the negative streamer zone after the streamer zone has been formed. This field is believed to be roughly equal to the stability field of negative streamer propagation [*Bazelyan and Raizer*, 2000, p. 69], that is $E_s^- \simeq 12.5$ kV/cm [*Babaeva and Naidis* 1997, Figure 7]. In this low field, attachment processes dominate over ionization processes, thus, in order to explain the continuous production of streamers once the streamer zone has been formed, as observed in experiments, the field right at the surface of the leader is believed to be approximately 50 kV/cm [*Bazelyan and Raizer*, 2000, p. 68]. The space charge field produced by the many propagating streamers forming the streamer zone during the negative corona flash lower the electric field down to $E_s^- \simeq 12.5$ kV/cm on a timescale of ~1 $\mu$s [e.g., *Moss et al.*, 2006]. The runaway electrons produced from streamer tips with energies of ~65 keV considered in this paper are able to further accelerate in the streamer zone. However, since streamers do not expand in such low fields, the production of very high electric fields in streamer heads is not sustained any longer (see section 3.3), and the production of runaway electrons from streamers is expected to cease after the negative corona flash has completed establishment of the new streamer zone with average electric field $E_s^- \simeq 12.5$ kV/cm.

[37] In the Monte Carlo calculations presented above, we introduced low-energy electrons (1 eV) at a rate of approximately $1.6 \times 10^{15}$ s$^{-1}$. Comparing this number to the typical frequency of runaway electrons we obtained in the simulations $1.4 \times 10^{13}$ s$^{-1}$, gives a probability of 1/120 for an electron to be a runaway among all of the electrons initially introduced in this system. In a streamer head, the conduction current is much lower than in the streamer channel, since the electron density drops fast in the charged region represented in Figure 2. Instead, the displacement current is high and we can consider an approximate continuity of the total current (i.e., conduction plus displacement) in all transversal sections of the streamer [*Vitello et al.*, 1994]. For this reason, the number of charges flowing through the streamer head is lower than that in the streamer channel. We have verified that the total electric current and the conduction current in the streamer head grow exponentially in time as the streamer propagates and expands. Extrapolation from our numerical results, such as those realized for potential distributions in section 3, and analytical estimates of the conduction current in the channel and displacement current in the head, both lead to a conduction current in the streamer head of $\gtrsim$100 A when the streamer radius reaches $R_s = 0.5$ cm. Note that the typical current of streamers produced in short laboratory gaps is ~1 A [e.g., *Celestin et al.*, 2008, Figure 9]. Since ions are much less mobile than electrons, we consider that only electrons participate in the production of the conduction current, and therefore the $\gtrsim$100 A of conduction current found in the streamer head corresponds to a frequency of passage of electrons through the streamer head of ~$10^{21}$ s$^{-1}$. Therefore, one obtains a frequency of runaway electrons emitted from the streamer of approximately $\nu_{run} \simeq 10^{19}$ s$^{-1}$, that is a factor of 500 greater than the emission rate derived previously from *Moss et al.* [2006]. We note that this difference mainly comes from two reasons. First, as we study the case of streamers with large radii, the flow of electrons (or electric current) in the streamer is naturally increased. Second, large radii involve smooth gradient of electric fields (see equations (4) and (5)) which are favorable to the emission of runaway electrons [see *Kunhardt and Byszewski*, 1980].

[38] The number of streamers present in a streamer zone of a leader at every moment of time can be approximated as $N_s = Q_s/q_s$, where $Q_s$ is the total charge in the streamer zone, and $q_s$ is the characteristic charge carried by a streamer [*Bazelyan and Raizer*, 2000, p. 70]. The quantity $Q_s$ is well approximated by the relation $Q_s = \pi\varepsilon_0 R_{sz}^- U_l$ and $q_s$ is generally on the order of 1 nC [*Bazelyan and Raizer*, 2000, p. 69–71]. As mentioned above, the size of the streamer zone of a negative leader is $R_{sz}^- = U_l/2E_s^-$, and therefore, for $U_l = 10$ MV and $E_s^- = 12.5$ kV/cm, one gets $R_{sz}^- = 4$ m and $Q_s \simeq 1$ mC. The number of streamers constituting the streamer zone of a lightning leader is then $N_s \simeq 10^6$. On the other hand, the characteristic time of production of runaway electrons by one streamer is related to the timescale over which the electric field in the streamer head can be higher than $E_c$. Both mechanisms discussed in section 3.3, that is the growth of electric field in the streamer head because of growth of streamer radius with respect to photoionization length or time rise of the applied voltage, would be on a timescale not much longer than 1 ns. Indeed, branching occurs on a timescale of 1 ns at ground pressure [e.g., *Liu and Pasko*, 2006], and the increase of the applied voltage produced from the negative leader tip during the negative corona flash is on the order of 10 ns (see section 5.1). Thus, if one consider that every streamer during the negative corona flash, eventually constituting the streamer zone of the negative leader, expands and produces energetic runaway electrons, the total number of runaway electrons produced is as high as $N_s \times \nu_{run} \times 10^{-9}$ s ~ $10^{16}$ which is in

agreement with the number of electrons estimated to be involved in the production of TGFs (~$10^{17}$) [*Dwyer and Smith*, 2005] without considering further amplification. This suggests that either a few e-foldings of electron multiplication in relativistic avalanches, or even no amplification at all in the low-electric fields present in thunderstorms, could explain the number of energetic photons measured from satellites. Indeed, electric fields typically measured in thunderstorms (~0.2 kV/cm [e.g., *Marshall et al.*, 1996, 2001]) are usually lower than the minimum electric field required to produce a relativistic runaway electron avalanche (~2 kV/cm at ground pressure, and ~0.3 kV/cm at 15 km altitude).

[39] We emphasize that TGFs have been correlated with +IC lightning discharges [*Stanley et al.*, 2006], and more recently, TGFs were found to occur within the initial milliseconds of compact +IC flashes while the negative leader developed upward [*Lu et al.*, 2010]. During this stage, the advancement of the negative lightning leader is believed to be made by the stepping processes [*Shao et al.*, 2010; *Lu et al.*, 2010]. In fact, *Shao et al.* [2010] have recently documented nine TGF-related lightning events observed by the Los Alamos Sferic Array. All TGF-related events detected by Los Alamos Sferic Array (LASA) were exclusively related to +IC discharges transporting electrons upward, whereas the majority of LASA's data were composed of cloud-to-ground (CG) return strokes. *Shao et al.* [2010] note that "TGFs appeared to be more closely related to precursor, small discharge pulses than to the triggering, main pulses. With a transmission line model and an assumption of $5 \times 10^7$ m/s for the current propagation speed for the individual impulsive events, the peak current for the TGF-related small pulses was estimated to be in the range of 3–19 kA, with most below 10 kA." In the work given by *Shao et al.* [2010], the heights of the TGF-related lightning pulses were estimated to be in the range of 10.5–14.1 km. Similarly, *Lu et al.* [2010] report the observation of a TGF-related lightning by the North Alabama Lightning Mapping Array. They estimated the lightning current corresponding to the occurrence of the TGF to be >5 kA by considering a leader channel of 2 km long, and found that the leader had ascended to an altitude of 10–11 km at the moment of the TGF production. Note that the recently observed TGF-related lightning leaders involve physical characteristics in agreement with those used in the previous paragraph in order to estimate the flux of energetic electrons given by the mechanism discussed in the present paper.

[40] After the initial phase of upward propagation of the main negative leader, the leader reaches the positively charged regions lying in the upper part of the thunderstorm. During this phase, negative leaders develop extensive branching and a horizontal spreading in this region [e.g., *Riousset et al.*, 2007]. One could believe that, since the lightning is highly branched, the detection of energetic radiation from one of these leader branches from satellites is even more likely. However, this seems to contradict the observations [*Shao et al.*, 2010; *Lu et al.*, 2010]. In fact, as stated above, the electric potential differences with respect to ambient potential on opposite ends of a straight lightning leader channel depend on both leader length $l_l$ and ambient electric field $E_{amb}$, and have a magnitude ~$l_l E_{amb}/2$. For typically low value of $E_{amb}$ cited earlier in our paper, the leader length $l_l$ should reach values on the order of several kilometers before production of tens of MeV electrons, whose radiation effects are observable from satellites, becomes possible. When the leader channel splits into branches, the total capacitance of the lightning leader is known to increase correspondingly [*Bazelyan and Raizer*, 2000, p. 166]. In fact, immediately after branching, the charge carried by each of the branches is lower than the charge on the original channel. Therefore, branching leads to a lower-potential differences of each of the branches with respect to the ambient potential and a reduction in peak total energy runaway electrons can achieve. We suggest that this mechanism is responsible for the extinction of TGFs at early stages of +IC discharges as soon as the original single negative leader with high-potential difference begins splitting in many branches. *Carlson et al.* [2010] have drawn similar conclusion on the extinction of TGFs due to extensive branching of the lightning leader. We emphasize that although the conclusion is similar, the argument put forward by *Carlson et al.* [2010] is based on the focusing of current in extensively branched leader channel networks, which is quite different from the idea of general decrease of the electric potential differences in the leader tips. The contributions of these mechanisms should be investigated further.

[41] As discussed above, the radius of the streamer zone is proportional to the potential difference $U_l$ between the leader tip potential and the ambient potential: $R_{sz}^- = U_l/2E_s^-$. The charge of the streamer zone is $Q_s = \pi\varepsilon_0 R_{sz}^- U_l$ [*Bazelyan and Raizer*, 2000, p. 69]. From those relations, one can explicitly write the charge of the streamer zone as a function of the potential in the leader tip:

$$Q_s = \frac{\pi\varepsilon_0 U_l^2}{2E_s^-} \tag{9}$$

The quadratic dependence of $Q_s$ on the potential in the leader tip is of great importance, since the number of energetic electrons generated from the leader is proportional to $Q_s$.

[42] Concerning the generation of X-rays from natural negative cloud-to-ground (−CG) lightning discharges, one needs to consider that the lightning consists of a network of branched leader channels. Because of branching, the individual branches of descending negative leaders form much lower-potential differences with respect to ambient potential [*Bazelyan and Raizer*, 2000, p. 166] and transport much lower values of charge than that expected in a single descending leader. For example, in the case of a typical potential of $U_l$ = 1 MV in the tips of −CG lightning leaders, the number of streamers is 100 times less than that in the case of unbranched +IC with $U_l$ = 10 MV discussed above. Moreover, as already noted above, the characteristic length in the streamer zone is proportional to $U_l$: $R_{sz}^- = U_l/2E_s^-$. In the case of $U_l$ = 1 MV, the size of the streamer zone would be $R_{sz}^- \simeq 40$ cm, and the high field region where streamers considerably expand during the negative corona flash (see Figure 8a), would be approximately 2.5 cm. We can calculate that although the potential drops of streamers with length of 2.5 cm are sufficiently high to generate runaway electrons, the flux of those electrons varying as $R_s^2$ would be significantly reduced by more than a factor of 10. This leads to a number of runaway electrons generated per pulse of ~$10^{13}$. *Dwyer et al.* [2010] demonstrated that measurements related to triggered lightning dart leaders by *Saleh et al.*

[2009] involved $10^{11}$ runaway electrons per pulse. We emphasize that the mechanisms of generation of X-rays by dart leaders can be quite different from that in the negative corona flashes of stepped leaders [see, e.g., *Cooray et al.*, 2009]. Furthermore, *Dwyer et al.* [2010] noted that "Measurements by TERA [Thunderstorm Energetic Radiation Array] have found that natural lightning stepped leaders are almost always much more intense in X rays than triggered (and natural) lightning dart or dart-stepped leaders, suggesting that this number of seed electrons [$10^{11}$] is probably on the low side for natural lightning." Thus, we consider that the processes of streamer expansion in the negative corona flashes discussed in this paper are also consistent with ground-based observations within 1 order of magnitude. We note that, even though the potential differences in leader tips of highly branched lightning is reduced, it is conceivable that the numerous leader branches, for example, at the end of IC lightnings [see, e.g., *Riousset et al.*, 2007], as well as the small precursors of lightning leaders could still generate an abundant quantity of low-flux energetic electrons, and corresponding X-rays in thunderclouds.

[43] The total number of energetic electrons from a streamer or a leader, or potential drops in streamers are invariant of pressure scaling [*Moss et al.*, 2006]. Concerning other physical parameters such as streamer lengths or timescales, the scaling factor $N_0/N$, where $N$ is the neutral density at a given altitude and $N_0$ is the neutral density at sea level, is ~3 at 10 km, and ~7 at 15 km. Although the models developed in this paper are quite advanced, the complexity of processes at play in the propagation of a negative leader only allows to make order of magnitude estimates. The scaling factors do not affect much physical characteristics discussed in this paper.

## 6. Conclusions

[44] Principal contributions of this work can be summarized as follows:

[45] 1. We have shown that the potential differences (drops) in a streamer head and in the region ahead of the streamer head increase exponentially when the streamer propagates in a field higher than the stability field.

[46] 2. From the exponential growth of the potential differences, we have been able to estimate the kinetic energy that runaway electrons can gain in the region of the streamer head.

[47] 3. Using a full energy range Monte Carlo model, we have shown that the runaway electrons emitted from negative streamers are able to reach energies as high as ~100 keV, with a peak probability corresponding to energy on the order of ~60 keV. The exact values of those quantities depend on the external conditions and on the mechanisms leading to high-electric field in the streamer head (growth of streamer radius with respect to photoionization length or time rise of the applied voltage).

[48] 4. Quantitative considerations on the electric fields produced by a negative leader have shown that runaway electrons with energies 60–100 keV are able to further accelerate and extract the few tens of MeVs of potential energy available in the leader tip fields.

[49] 5. We have obtained a flux of energetic electrons from streamers and from negative corona flashes consistent with the typical number of energetic electrons (~$10^{17}$) involved in production of TGFs without the need for additional amplification in relativistic runaway electron avalanche process.

[50] 6. We have suggested that the production of energetic electrons from negative leaders stops when significant branching of the leader develops, since branching process results in lower-potential differences of the leader branches with respect to ambient potential. This suggestion is consistent with recent measurements showing that TGFs occur within the initial milliseconds of compact +IC flashes while the negative leaders developed upward.

[51] **Acknowledgments.** This research was supported by the NSF grants AGS-0734083 and AGS-0741589 to Penn State University.

[52] Robert Lysak thanks the reviewers for their assistance in evaluating this paper.

## References

Babaeva, N. Y., and G. V. Naidis (1997), Dynamics of positive and negative streamers in air in weak uniform electric fields, *IEEE Trans. Plasma Sci.*, *25*, 375, doi:10.1109/27.602514.

Babich, L. P. (1982), A new type of ionization wave and the mechanism of polarization self-acceleration of electrons in gas discharges at high overvoltages, *Sov. Phys. Dokl., Engl. Transl.*, *27*, 215.

Balanis, C. A. (1989), *Advanced Engineering Electromagnetics*, John Wiley, New York.

Bazelyan, E. M., and Y. P. Raizer (2000), *Lightning Physics and Lightning Protection*, IoP Ltd., Bristol, U. K.

Bourdon, A., V. P. Pasko, N. Y. Liu, S. Celestin, P. Ségur, and E. Marode (2007), Efficient models for photoionization produced by non-thermal gas discharges in air based on radiative transfer and the Helmholtz equations, *Plasma Sources Sci. Technol.*, *16*, 656.

Briggs, M. S., et al. (2010), First results on terrestrial gamma ray flashes from the Fermi Gamma-ray Burst Monitor, *J. Geophys. Res.*, *115*, A07323, doi:10.1029/2009JA015242.

Carlson, B. E., N. G. Lehtinen, and U. S. Inan (2007), Constraints on terrestrial gamma ray flash production from satellite observation, *Geophys. Res. Lett.*, *34*, L08809, doi:10.1029/2006GL029229.

Carlson, B. E., N. G. Lehtinen, and U. S. Inan (2009), Terrestrial gamma ray flash production by lightning current pulses, *J. Geophys. Res.*, *114*, A00E08, doi:10.1029/2009JA014531.

Carlson, B. E., N. G. Lehtinen, and U. S. Inan (2010), Terrestrial gamma ray flash production by active lightning leader channels, *J. Geophys. Res.*, *115*, A10324, doi:10.1029/2010JA015647.

Celestin, S., and V. P. Pasko (2010a), Monte Carlo models for studies of electron runaway phenomena in air, *W2 ECCR24*, CEDAR Workshop, Univ. of Colo. at Boulder, Boulder, 20–25 June.

Celestin, S., and V. P. Pasko (2010b), Effects of spatial non-uniformity of streamer discharges on spectroscopic diagnostics of peak electric fields in transient luminous events, *Geophys. Res. Lett.*, *37*, L07804, doi:10.1029/2010GL042675.

Celestin, S., and V. P. Pasko (2010c), Soft collisions in relativistic runaway electron avalanches, *J. Phys. D Appl. Phys.*, *43*, 315206, doi:10.1088/0022-3727/43/31/315206.

Celestin, S., G. Canes-Boussard, O. Guaitella, A. Bourdon, and A. Rousseau (2008), Influence of the charges deposition on the spatio-temporal self-organization of streamers in a DBD, *J. Phys. D Appl. Phys.*, *41*, 205214.

Colman, J. J., R. A. Roussel-Dupré, and L. Triplett (2010), Temporally self-similar electron distribution functions in atmospheric breakdown: The thermal runaway regime, *J. Geophys. Res.*, *115*, A00E16, doi:10.1029/2009JA014509.

Cooray, V., M. Becerra, and V. Rakov (2009), On the electric field at the tip of dart leaders in lightning flashes, *J. Atmos. Sol. Terr. Phys.*, *71*(12), 1397, doi:10.1016/j.jastp.2009.06.002.

Cummer, S. A., Y. Zhai, W. Hu, D. M. Smith, L. I. Lopez, and M. A. Stanley (2005), Measurements and implications of the relationship between lightning and terrestrial gamma ray flashes, *Geophys. Res. Lett.*, *32*, L08811, doi:10.1029/2005GL022778.

Dwyer, J. R. (2003), A fundamental limit on electric fields in air, *Geophys. Res. Lett.*, *30*(20), 2055, doi:10.1029/2003GL017781.

Dwyer, J. R. (2008), Source mechanisms of terrestrial gamma-ray flashes, *J. Geophys. Res.*, *113*, D10103, doi:10.1029/2007JD009248.

Dwyer, J. R. (2010), Diffusion of relativistic runaway electrons and implications for lightning initiation, *J. Geophys. Res.*, *115*, A00E14, doi:10.1029/2009JA014504.

Dwyer, J. R., and D. M. Smith (2005), A comparison between Monte Carlo simulations of runaway breakdown and terrestrial gamma-ray flash observations, *Geophys. Res. Lett.*, *32*, L22804, doi:10.1029/2005GL023848.

Dwyer, J. R., et al. (2003), Energetic radiation during rocket-triggered lightning, *Science*, *299*(5607), 694, doi:10.1126/science.1078940.

Dwyer, J. R., et al. (2004a), Measurements of X-ray emission from rocket-triggered lightning, *Geophys. Res. Lett.*, *31*, L05118, doi:10.1029/2003GL018770.

Dwyer, J. R., et al. (2004b), A ground level gamma-ray burst observed in association with rocket-triggered lightning, *Geophys. Res. Lett.*, *31*, L05119, doi:10.1029/2003GL018771.

Dwyer, J. R., et al. (2005), X-ray bursts associated with leader steps in cloud-to-ground lightning, *Geophys. Res. Lett.*, *32*, L01803, doi:10.1029/2004GL021782.

Dwyer, J. R., D. M. Smith, M. A. Uman, Z. Saleh, B. Grefenstette, B. Hazelton, and H. K. Rassoul (2010), Estimation of the fluence of high-energy electron bursts produced by thunderclouds and the resulting radiation doses received in aircraft, *J. Geophys. Res.*, *115*, D09206, doi:10.1029/2009JD012039.

Dyakonov, M. I., and V. Y. Kachorovskii (1988), Theory of streamer discharge in semiconductors, *Sov. Phys. JETP, Engl. Transl.*, *67*, 1049.

Dyakonov, M. I., and V. Y. Kachorovskii (1989), Streamer discharge in a homogeneous field, *Sov. Phys. JETP, Engl. Transl.*, *68*, 1070.

Fishman, G. J., and D. M. Smith (2008), Observations of two terrestrial gamma-ray flashes (TGFs) over a wide energy range with the Fermi Gamma-ray Burst Monitor, *Eos Trans. AGU*, *89*(53), Fall Meet. Suppl., Abstract AE21A-02.

Fishman, G., et al. (1994), Discovery of intense gamma-ray flashes of atmospheric origin, *Science*, *264*(5163), 1313.

Fuschino, F., et al. (2009), AGILE view of TGFs, *AIP Conf. Proc.*, *1118*(1), 46, doi:10.1063/1.3137712.

Grefenstette, B. W., D. M. Smith, J. R. Dwyer, and G. J. Fishman (2008), Time evolution of terrestrial gamma ray flashes, *Geophys. Res. Lett.*, *35*, L06802, doi:10.1029/2007GL032922.

Gurevich, A. V. (1961), On the theory of runaway electrons, *Sov. Phys. JETP, Engl. Transl.*, *12*, 904.

Gurevich, A. V., and K. P. Zybin (2001), Runaway breakdown and electric discharges in thunderstorms, *Phys. Uspekhi*, *44*(11), 1119.

Gurevich, A. V., and K. P. Zybin (2005), Runaway breakdown and the mysteries of lightning, *Phys. Today*, *58*(5), 37, doi:10.1063/1.1995746.

Gurevich, A. V., G. M. Milikh, and R. A. Roussel-Dupré (1992), Runaway electron mechanism of air breakdown and preconditioning during a thunderstorm, *Phys. Lett. A.*, *165*, 463, doi:10.1016/0375-9601(92)90348-P.

Gurevich, A. V., Y. V. Medvedev, and K. P. Zybin (2004), Thermal electrons and electric current generated by runaway breakdown effect, *Phys. Lett. A.*, *321*, 179, doi:10.1016/j.physleta.2003.10.062.

Hagelaar, G. J. M., and L. C. Pitchford (2005), Solving the Boltzmann equation to obtain electron transport coefficients and rate coefficients for fluid models, *Plasma Sources Sci. Technol.*, *14*, 722.

Hazelton, B. J., B. W. Grefenstette, D. M. Smith, J. R. Dwyer, X. Shao, S. A. Cummer, T. Chronis, E. H. Lay, and R. H. Holzworth (2009), Spectral dependence of terrestrial gamma-ray flashes on source distance, *Geophys. Res. Lett.*, *36*, L01108, doi:10.1029/2008GL035906.

Kambara, H., and K. Kuchitsu (1972), Measurement of differential cross sections of low-energy electrons elastically scattered by gas molecules. I. Apparatus, *Jpn. J. Appl. Phys.*, *11*, 609, doi:10.1143/JJAP.11.609.

Kim, Y.-K., J. P. Santos, and F. Parente (2000), Extension of the binary-encounter-dipole model to relativistic incident electrons, *Phys. Rev. A*, *62*, 052710, doi:10.1103/PhysRevA.62.052710.

Krehbiel, P. R., J. A. Riousset, V. P. Pasko, R. J. Thomas, W. Rison, M. A. Stanley, and H. E. Edens (2008), Upward electrical discharges from thunderstorms, *Nature Geosci.*, *1*(4), 233.

Kulikovsky, A. A. (1995), Two-dimensional simulation of the positive streamer in $N_2$ between parallel-plate electrodes, *J. Phys. D Appl. Phys.*, *28*, 2483.

Kulikovsky, A. A. (1997a), Positive streamer between parallel plate electrodes in atmospheric pressure air, *J. Phys. D Appl. Phys.*, *30*, 441.

Kulikovsky, A. A. (1997b), The mechanism of positive streamer acceleration and expansion in air in a strong external field, *J. Phys. D Appl. Phys.*, *30*, 1515.

Kunhardt, E. E., and W. W. Byszewski (1980), Development of overvoltage breakdown at high gas pressure, *Phys. Rev. A*, *21*, 2069, doi:10.1103/PhysRevA.21.2069.

Kunhardt, E. E., Y. Tzeng, and J. P. Boeuf (1986), Stochastic development of an electron avalanche, *Phys. Rev. A*, *34*, 440, doi:10.1103/PhysRevA.34.440.

Kuo, C.-L., et al. (2009), Discharge processes, electric field, and electron energy in ISUAL-recorded gigantic jets, *J. Geophys. Res.*, *114*, A04314, doi:10.1029/2008JA013791.

Kyuregyan, A. S. (2008), Asymptotically self-similar propagation of spherical ionization waves, *Phys. Rev. Lett.*, *101*, 174505, doi:10.1103/PhysRevLett.101.174505.

Lehtinen, N. G., T. F. Bell, and U. S. Inan (1999), Monte Carlo simulation of runaway MeV electron breakdown with application to red sprites and terrestrial gamma ray flashes, *J. Geophys. Res.*, *104*, 24,699, doi:10.1029/1999JA900335.

Liu, N., and V. P. Pasko (2004), Effects of photoionization on propagation and branching of positive and negative streamers in sprites, *J. Geophys. Res.*, *109*, A04301, doi:10.1029/2003JA010064.

Liu, N., and V. P. Pasko (2006), Effects of photoionization on similarity properties of streamers at various pressures in air, *J. Phys. D Appl. Phys.*, *39*, 327.

Liu, N., S. Celestin, A. Bourdon, V. P. Pasko, P. Ségur, and E. Marode (2007), Application of photoionization models based on radiative transfer and the Helmholtz equations to studies of streamers in weak electric fields, *Appl. Phys. Lett.*, *91*(21), 211501, doi:10.1063/1.2816906.

Liu, N. Y., V. P. Pasko, K. Adams, H. C. Stenbaek-Nielsen, and M. G. McHarg (2009), Comparison of acceleration, expansion, and brightness of sprite streamers obtained from modeling and high-speed video observations, *J. Geophys. Res.*, *114*, A00E03, doi:10.1029/2008JA013720.

Lu, G., R. J. Blakeslee, J. Li, D. M. Smith, X. Shao, E. W. McCaul, D. E. Buechler, H. J. Christian, J. M. Hall, and S. A. Cummer (2010), Lightning mapping observation of a terrestrial gamma-ray flash, *Geophys. Res. Lett.*, *37*, L11806, doi:10.1029/2010GL043494.

March, V., and J. Montanyà (2010), Influence of the voltage-time derivative in X-ray emission from laboratory sparks, *Geophys. Res. Lett.*, *37*, L19801, doi:10.1029/2010GL044543.

Marisaldi, M., et al. (2010), Detection of terrestrial gamma ray flashes up to 40 MeV by the AGILE satellite, *J. Geophys. Res.*, *115*, A00E13, doi:10.1029/2009JA014502.

Marshall, T. C., M. Stolzenburg, and W. D. Rust (1996), Electric field measurements above mesoscale convective systems, *J. Geophys. Res.*, *101*, 6979, doi:10.1029/95JD03764.

Marshall, T. C., M. Stolzenburg, W. D. Rust, E. R. Williams, and R. Boldi (2001), Positive charge in the stratiform cloud of a mesoscale convective system, *J. Geophys. Res.*, *106*, 1157, doi:10.1029/2000JD900625.

McHarg, M. G., H. C. Stenbaek-Nielsen, T. Kanmae, and R. K. Haaland (2010), Streamer tip splitting in sprites, *J. Geophys. Res.*, *115*, A00E53, doi:10.1029/2009JA014850.

Moore, C. B., K. B. Eack, G. D. Aulich, and W. Rison (2001), Energetic radiation associated with lightning stepped-leaders, *Geophys. Res. Lett.*, *28*, 2141, doi:10.1029/2001GL013140.

Morrow, R., and J. J. Lowke (1997), Streamer propagation in air, *J. Phys. D Appl. Phys.*, *30*, 614.

Moss, G. D., V. P. Pasko, N. Liu, and G. Veronis (2006), Monte Carlo model for analysis of thermal runaway electrons in streamer tips in transient luminous events and streamer zones of lightning leaders, *J. Geophys. Res.*, *111*, A02307, doi:10.1029/2005JA011350.

Murphy, T. (1988), Total and differential electron collision cross sections for $O_2$ and $N_2$, *Rep. LA-11288-MS*, Los Alamos Natl. Lab., Los Alamos, N. M.

Naidis, G. V. (1996), Dynamics of high-frequency streamers in air, *J. Exp. Theor. Phys.*, *82*, 694.

Nguyen, C. V., A. P. J. van Deursen, and U. Ebert (2008), Multiple X-ray bursts from long discharges in air, *J. Phys. D Appl. Phys.*, *41*, 234012.

Nguyen, C. V., A. P. J. van Deursen, E. J. M. van Heesch, G. J. J. Winands, and A. J. M. Pemen (2010), X-ray emission in streamer-corona plasma, *J. Phys. D Appl. Phys.*, *43*, 025202.

Østgaard, N., T. Gjesteland, J. Stadsnes, P. H. Connell, and B. Carlson (2008), Production altitude and time delays of the terrestrial gamma flashes: Revisiting the Burst and Transient Source Experiment spectra, *J. Geophys. Res.*, *113*, A02307, doi:10.1029/2007JA012618.

Petrov, N. I., and F. D'Alessandro (2002), Theoretical analysis of the processes involved in lightning attachment to earthed structures, *J. Phys. D Appl. Phys.*, *35*, 1788, doi:10.1088/0022-3727/35/14/321.

Rahman, M., V. Cooray, N. A. Ahmad, J. Nyberg, V. A. Rakov, and S. Sharma (2008), X rays from 80-cm long sparks in air, *Geophys. Res. Lett.*, *35*, L06805, doi:10.1029/2007GL032678.

Raizer, Y. P. (1991), *Gas Discharge Physics*, Springer, New York.

Rakov, V. A., and M. A. Uman (2003), *Lightning: Physics and Effects*, Cambridge Univ. Press, Cambridge, U. K.

Riousset, J. A. (2006), Fractal modeling of lightning discharges, M.S. thesis, Pa. State Univ., University Park.

Riousset, J. A., V. P. Pasko, P. R. Krehbiel, R. J. Thomas, and W. Rison (2007), Three-dimensional fractal modeling of intracloud lightning dis-

charge in a New Mexico thunderstorm and comparison with lightning mapping observations, *J. Geophys. Res.*, *112*, D15203, doi:10.1029/2006JD007621.

Roussel-Dupré, R. A., A. V. Gurevich, T. Tunnel, and G. M. Milikh (1994), Kinetic theory of runaway breakdown, *Phys. Rev. E*, *49*, 2257, doi:10.1103/PhysRevE.49.2257.

Saleh, Z., J. Dwyer, J. Howard, M. Uman, M. Bakhtiari, D. Concha, M. Stapleton, D. Hill, C. Biagi, and H. Rassoul (2009), Properties of the X-ray emission from rocket-triggered lightning as measured by the Thunderstorm Energetic Radiation Array (TERA), *J. Geophys. Res.*, *114*, D17210, doi:10.1029/2008JD011618.

Shao, X., T. Hamlin, and D. M. Smith (2010), A closer examination of terrestrial gamma-ray flash-related lightning processes, *J. Geophys. Res.*, *115*, A00E30, doi:10.1029/2009JA014835.

Shyn, T. W., R. S. Stolarski, and G. R. Carignan (1972), Angular distribution of electrons elastically scattered from $N_2$, *Phys. Rev. A*, *6*, 1002, doi:10.1103/PhysRevA.6.1002.

Smith, D. M., L. I. Lopez, R. P. Lin, and C. P. Barrington-Leigh (2005), Terrestrial gamma-ray flashes observed up to 20 MeV, *Science*, *307*, 1085.

Smith, D. M., B. J. Hazelton, B. W. Grefenstette, J. R. Dwyer, R. H. Holzworth, and E. H. Lay (2010), Terrestrial gamma ray flashes correlated to storm phase and tropopause height, *J. Geophys. Res.*, *115*, A00E49, doi:10.1029/2009JA014853.

Stanley, M. A., X.-M. Shao, D. M. Smith, L. I. Lopez, M. B. Pongratz, J. D. Harlin, M. Stock, and A. Regan (2006), A link between terrestrial gamma-ray flashes and intracloud lightning discharges, *Geophys. Res. Lett.*, *33*, L06803, doi:10.1029/2005GL025537.

Vitello, P. A., B. M. Penetrante, and J. N. Bardsley (1994), Simulation of negative-streamer dynamics in nitrogen, *Phys. Rev. E*, *49*, 5574, doi:10.1103/PhysRevE.49.5574.

S. Celestin and V. P. Pasko, Department of Electrical Engineering, Communications and Space Sciences Laboratory, Pennsylvania State University, 227 Electrical Engineering East, University Park, PA 16802-2706, USA. (sebastien.celestin@psu.edu; vpasko@psu.edu)